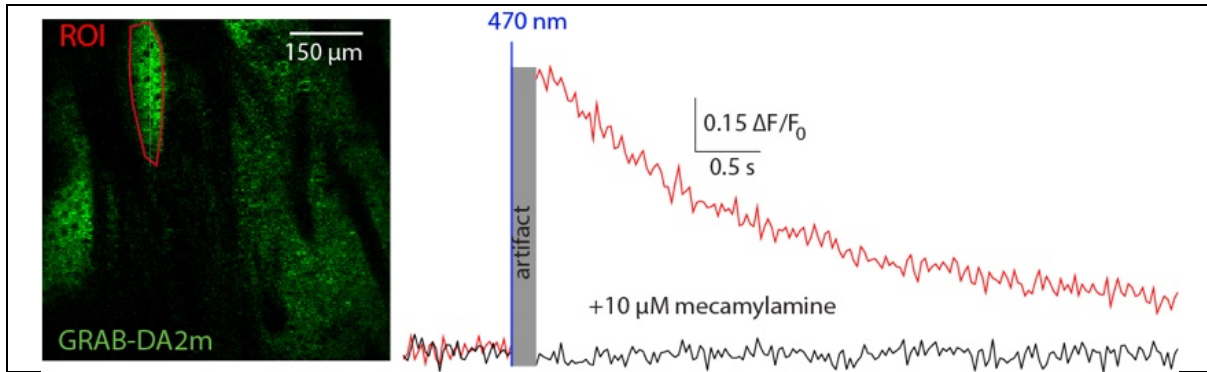
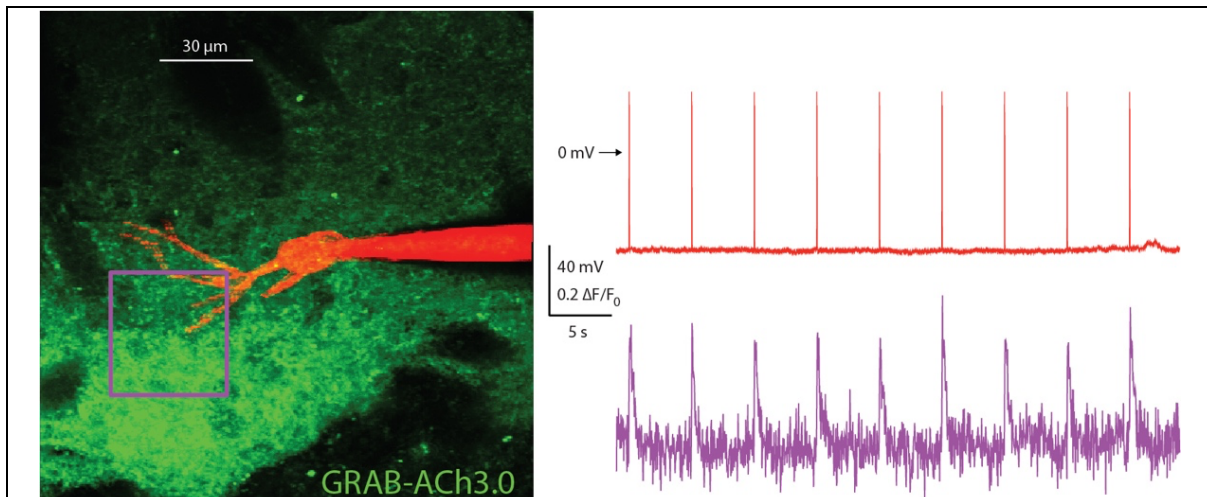


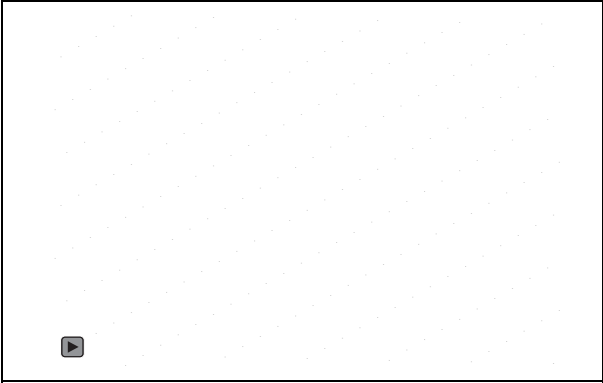
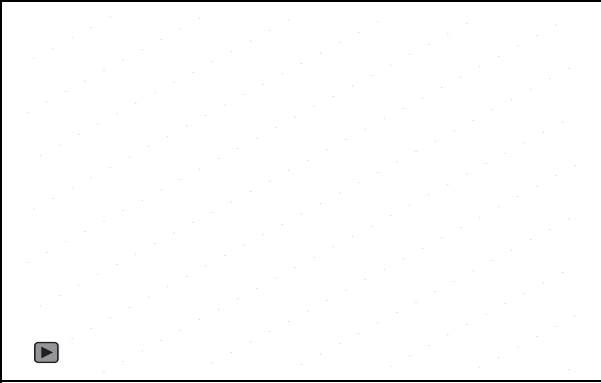
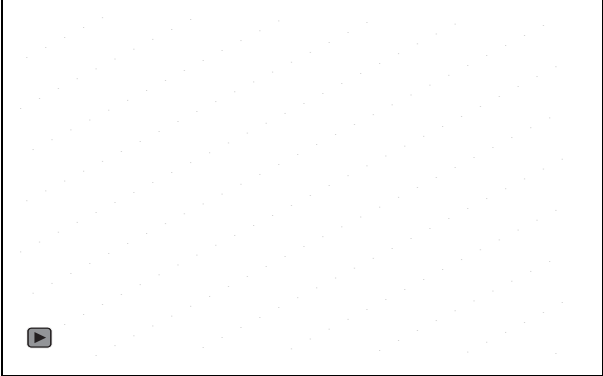
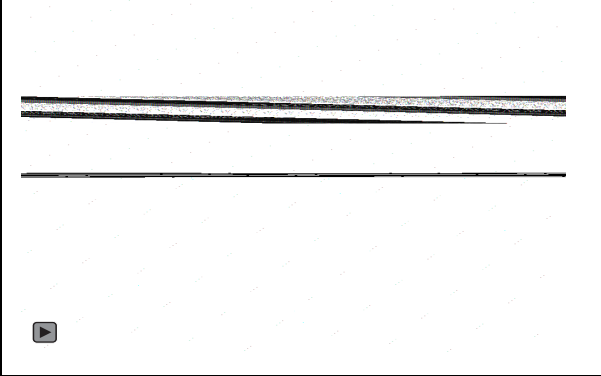
**Supplementary Fig. 1:** **a.** Distributions of wave durations and inter-wave intervals pooled from individual mice imaged with GRAB-ACh3.0. **b.** Distributions of wave durations and inter-wave intervals pooled from individual mice (1-3) imaged with iAChSnFR. **c.** Distributions of wave durations and inter-wave intervals pooled from mice 4-6 imaged with iAChSnFR. **d.** Distributions of wave velocities pooled from mice 4-6 imaged with iAChSnFR. Source data are provided as a Source Data file.

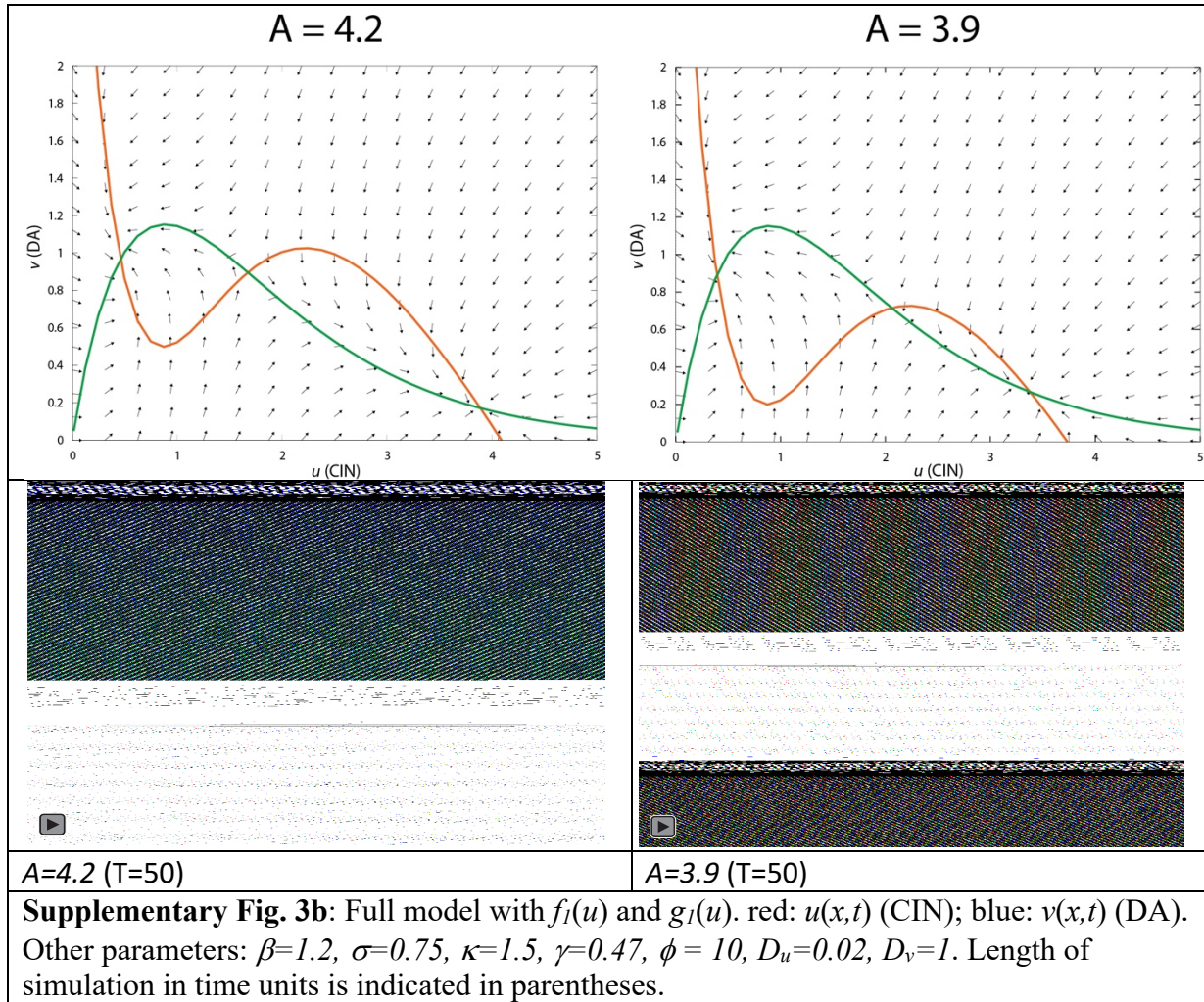


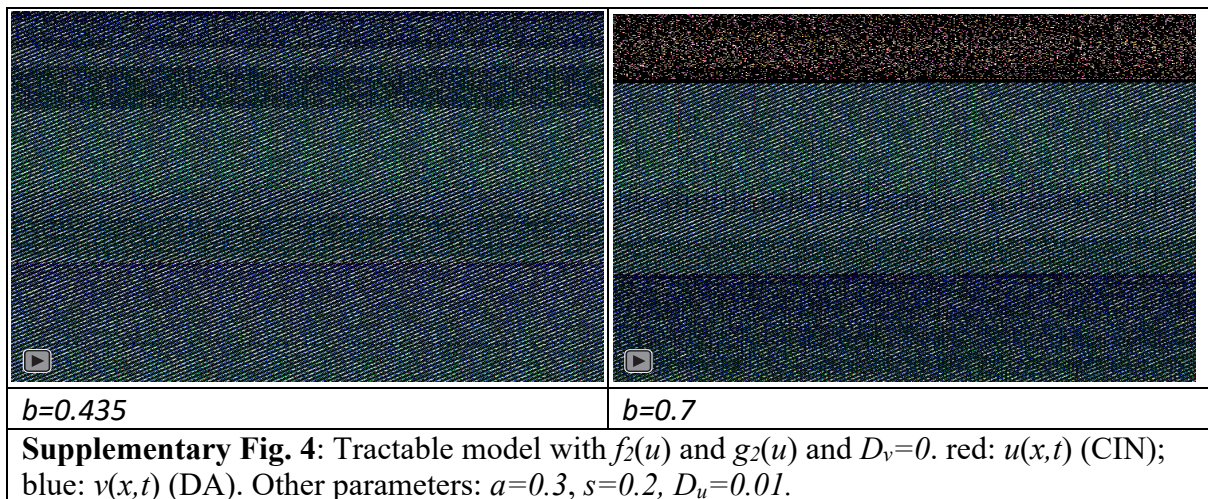
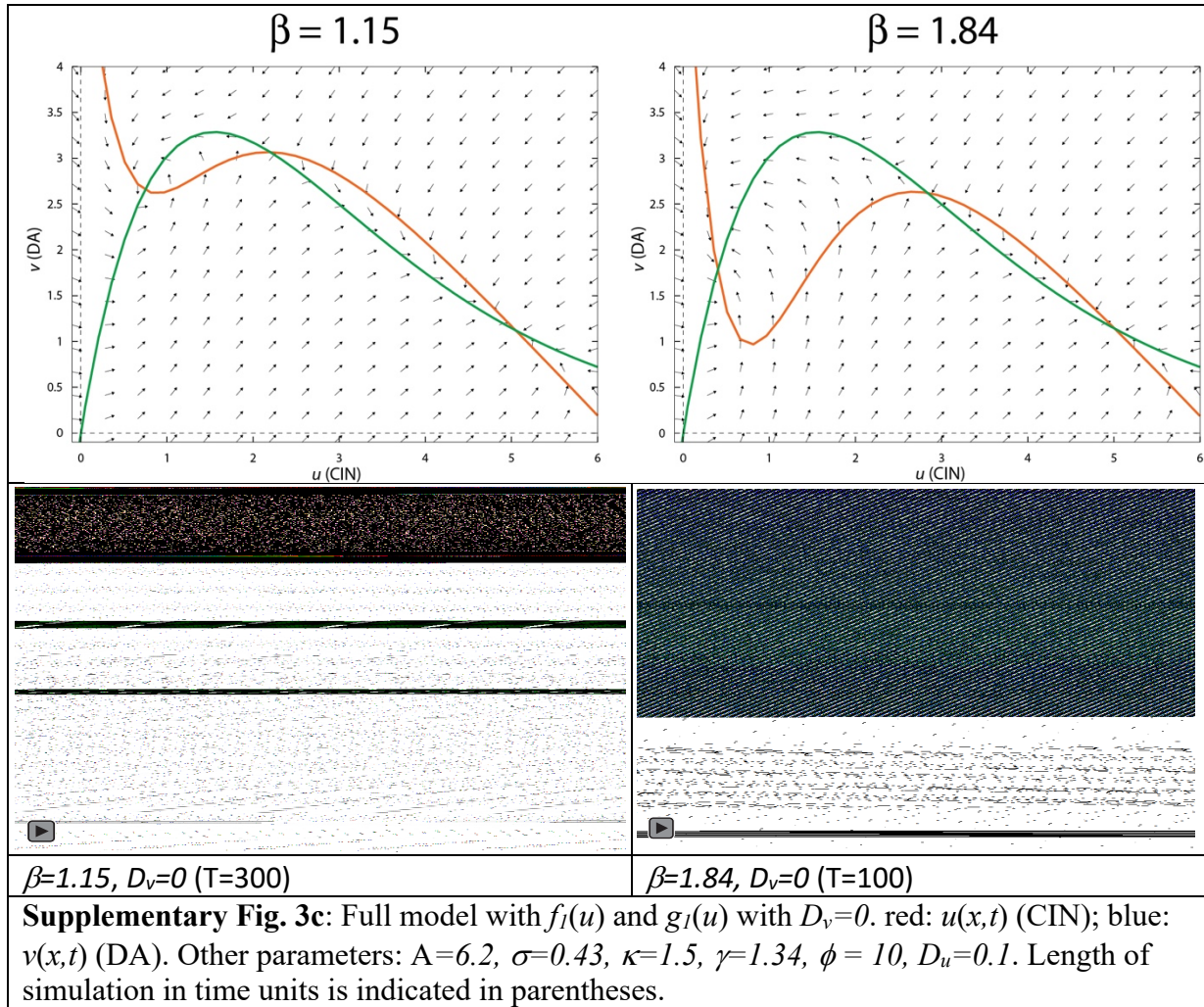
**Supplementary Fig. 2a:** Synchronous optogenetic activation (with a 1-ms long, 470 nm pulse) of CINs in an acute slice from a ChAT-ChR2 mouse whose dorsal striatum was inoculated with AAVs harboring GRAB-DA2m, causes DA release that is eliminated in the presence of 10  $\mu\text{M}$  mecamylamine, a nAChR antagonist. DA release was evoked in 8 slices from 4 mice, and the mecamylamine block was tested and confirmed in 3 slices from two of these mice. The artifact which is removed is explained in the Methods section.

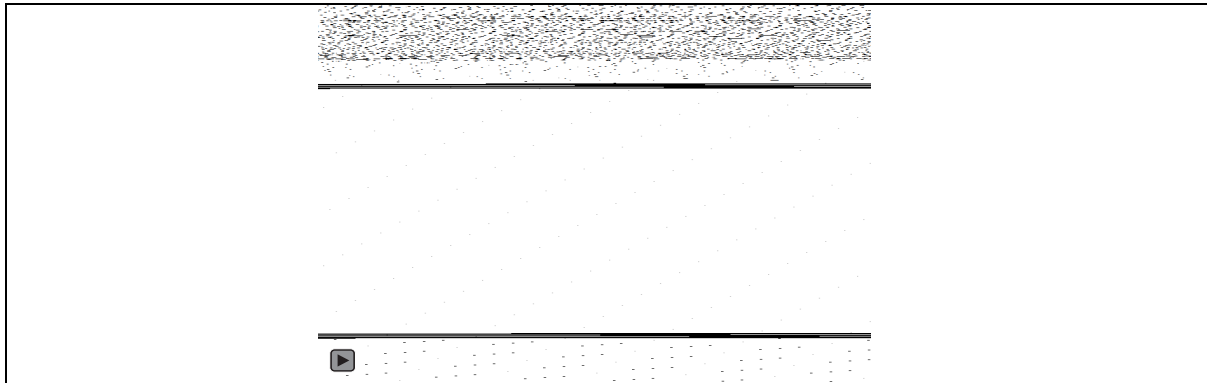


**Supplementary Fig. 2b:** Nine action potentials were elicited in an individual CIN hyperpolarized to quiescence (each with a 35 ms-long, 220 pA current pulse). The action potentials triggered ACh release (averaged from the color coded box) as visualized in wild-type mice whose dorsal striatum was inoculated with GRAB-ACh3.0. At this frequency (0.2 Hz) the median decrease of the amplitude of the 2<sup>nd</sup> to 9<sup>th</sup> ACh responses was no more than 4% relative to the 1<sup>st</sup> response ( $n = 4$  CINs from  $N = 3$  mice).

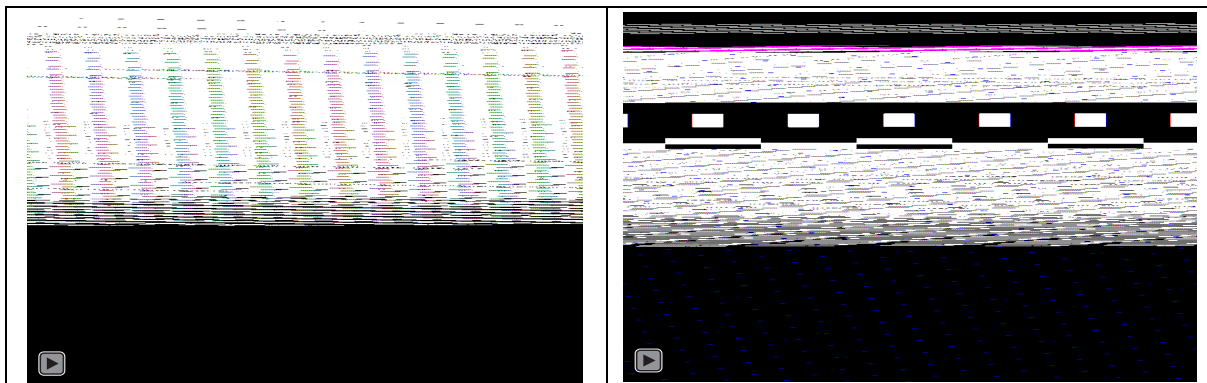
	
$\beta=1, D_u=0.02$ (T=50)	$\beta=1.8, D_u=0.02$ (T=50)
	
$\beta=1, D_u=1$ (T=10)	$\beta=1.8, D_u=1$ (T=10)
<p><b>Supplementary Fig. 3a:</b> Full model with <math>f_i(u)</math> and <math>g_i(u)</math>. red: <math>u(x,t)</math> (CIN); blue: <math>v(x,t)</math> (DA). Other parameters: <math>A=4.2</math>, <math>\sigma=0.75</math>, <math>\kappa=1.5</math>, <math>\gamma=0.47</math>, <math>\phi = 10</math>, <math>D_v=1</math>. Length of simulation in time units is indicated in parentheses.</p>	







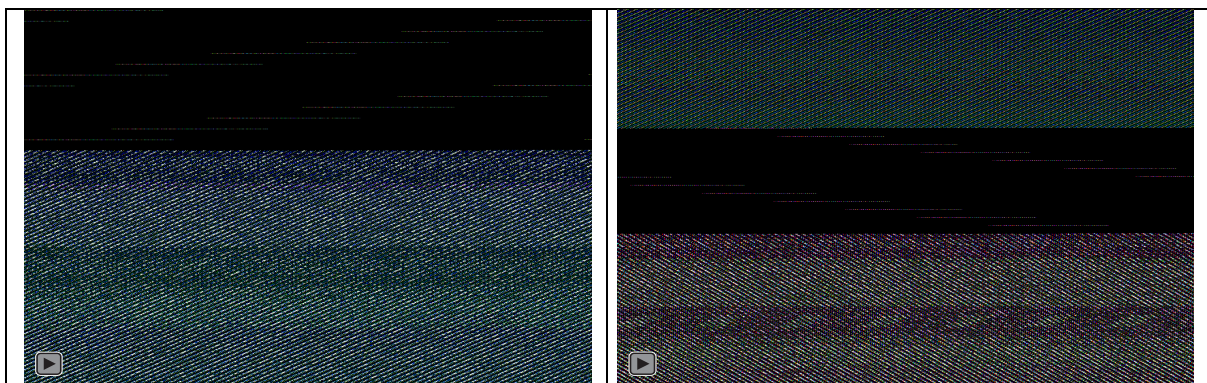
**Supplementary Fig. 5:** Turing instability in tractable model with  $f_2(u)$  and  $g_2(u)$ . red:  $u(x,t)$  (CIN); blue:  $v(x,t)$  (DA). Other parameters:  $a=0.3$ ,  $b=0.435$ ,  $s=0.2$ ,  $D_u=0.06$ ,  $D_v=1$ .



$v(x_o, t=20) = 15$

$v(x_o, t=20) = 20$

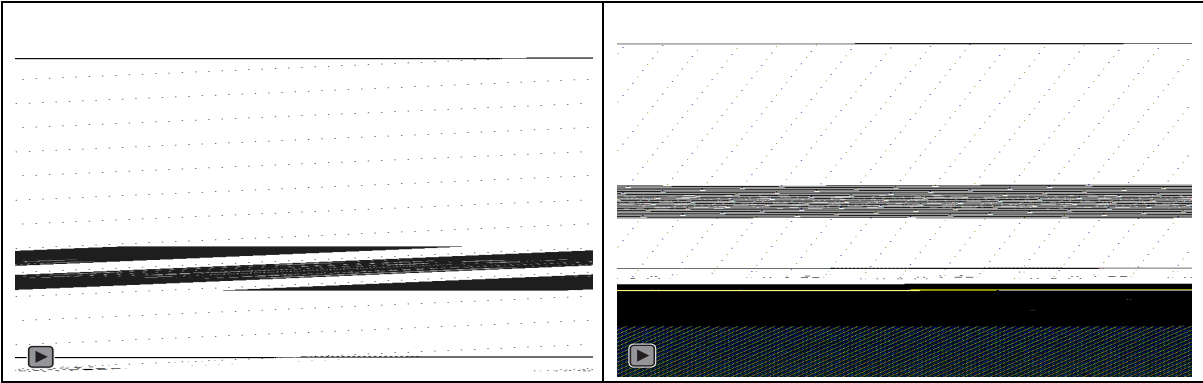
**Supplementary Fig 6a.** Response to transient local activation of  $v$  (DA) in full model with  $f_1(u)$  and  $g_1(u)$ . red:  $u(x,t)$  (CIN); blue:  $v(x,t)$  (DA). Other parameters:  $A=3.9$ ,  $\beta=1.2$ ,  $\sigma=0.75$ ,  $\kappa=1.5$ ,  $\gamma=0.47$ ,  $\phi = 10$ ,  $D_u=0.01$ ,  $D_v=1$ .



$u(x_o, t=5) = 10$

$u(x_o, t=5) = 20$

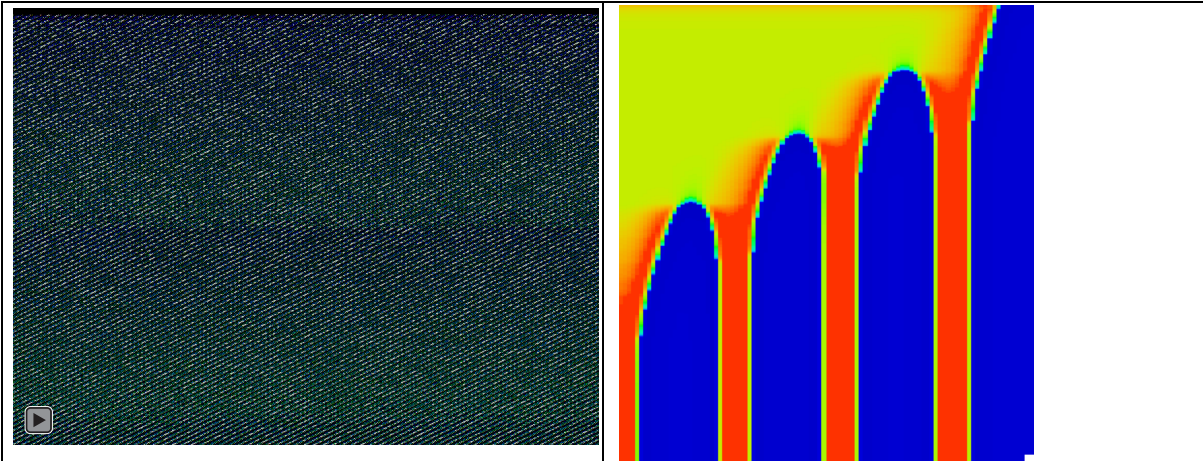
**Supplementary Fig 6b.** Response to transient local activation of  $u$  (CIN) in full model with  $f_1(u)$  and  $g_1(u)$ . red:  $u(x,t)$  (CIN); blue:  $v(x,t)$  (DA). Other parameters:  $A=4.3$ ,  $\beta=1.2$ ,  $\sigma=0.75$ ,  $\kappa=1.5$ ,  $\gamma=0.47$ ,  $\phi = 10$ ,  $D_u=0.01$ ,  $D_v=1$ .



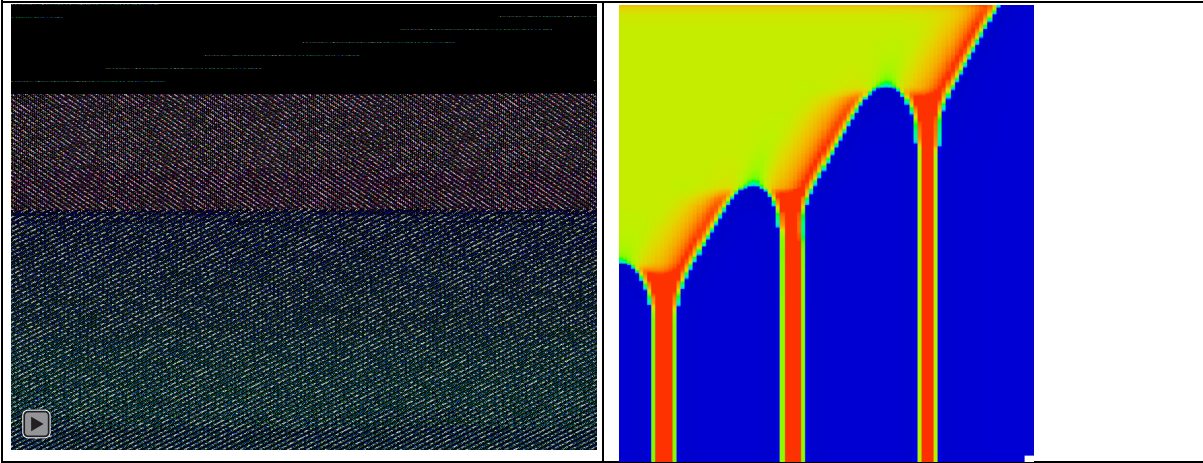
$\beta=1.35$

$\beta=1.55$

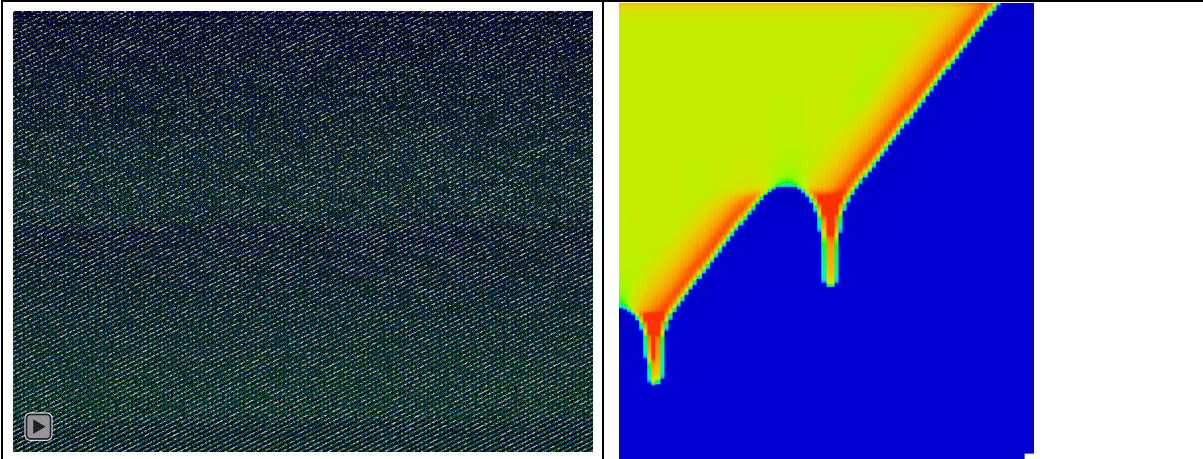
**Supplementary Fig 7.** Full model with  $f_I(u)$  and  $g_I(u)$  with  $\sigma=0.1$ . red:  $u(x,t)$  (CIN); blue:  $v(x,t)$  (DA). Other parameters:  $A=4.3$ ,  $\kappa=1.5$ ,  $\gamma=0.47$ ,  $\phi = 10$ ,  $D_u=0.2$ ,  $D_v=1$ .



$D_u=0.01$



$D_u=0.015$



$D_u=0.02$

**Supplementary Fig. 8:** Stable and unstable Turing patterns in full model with  $f_I(u)$  and  $g_I(u)$ . red:  $u(x,t)$  (CIN); blue:  $v(x,t)$  (DA). Other parameters:  $A=4.3$ ,  $\beta=1.62$ ,  $\sigma=0.1$ ,  $\kappa=1.5$ ,  $\gamma=0.5$ ,  $D_v=1$ .



